EPJ Web of Conferences **318**, 03004 (2025) https://doi.org/10.1051/epjconf/202531803004
AAPM-III 2025

Variation of metal corrosion rate during cyclic loading in potential failure zones

Anton Tyusenkov, *Darina* Abramovskikh, *Jamshed* Shermatov, *Valeriya* Pudakova*, and *Alexey* Rubtsov

Ufa State Petroleum Technological University, Department Technological machines and equipment, Ufa, 450064, Russian Federation

Abstract. Technological equipment of oil and gas processing under certain technological processes is simultaneously operated both in conditions of corrosive working media and in cyclic loading mode. Under such conditions, the probability of premature destruction increases significantly. Corrosion wear contributes to the exhaustion of the safety margin, and cyclic loading contributes to the formation of fatigue cracks. Regulatory documents regulate control methods for detecting the degree of corrosion wear and fatigue cracks. However, the most interesting scientific topic is the study of the relationship between the rate of metal corrosion and the level of accumulated damage in the aggregate. Therefore, research on the development of new methods, as well as diagnostic features to determine the zones of possible destruction under operating conditions of objects with simultaneous exposure to corrosion wear and cyclic loading, is relevant. The authors suggest that in metal zones with the maximum level of accumulated damage, the corrosion rate may be the most intense.

1 Introduction

One of the dominant mechanisms of damage to process equipment during operation is corrosion wear, as well as cyclic loading [1-3]. Moreover, in most cases, the above damage mechanisms are cumulative. As a result of simultaneous exposure of the equipment material to corrosive media and cyclic loads, its irreversible degradation and gradual accumulation of damage at micro- and macroscopic levels occur [4-5]. When a critical level of damage is accumulated, a certain zone or element of equipment is destroyed. Various authors have conducted research in the field of studying the regularities of metal corrosion in various conditions and obtained new scientific results [6-7].

However, the problem of identifying the locations of possible destruction of process equipment and predicting the time to destruction while taking into account corrosion and metal fatigue with sufficient accuracy to the end remains unresolved. Therefore, research on the development of new methods for identifying zones of possible destruction in process equipment during operation is relevant.

* Corresponding author: Pudakova.lera@yandex.ru

2 Research methodology

In order to investigate the corrosion rate trend of steel 09G2S with different levels of accumulated damage, low cycle fatigue tests were carried out in the first stage. For testing, flat samples with established dimensions were made in accordance with the current regulatory and technical documentation.

The samples were tested on a fatigue machine according to the symmetrical net bending scheme in accordance with the requirements of regulatory documents. An example of a flat test specimen is shown in Figure 1.

Fig. 1. Example of a flat sample for low cycle fatigue tests.

After cyclic loading of the samples, polarization studies were carried out to determine the corrosion rate at individual points. Measurements were made at 11 points on the surface of the samples (Figure 1).

Fig. 2. Corrosion rate measurement points.

The studies were carried out in a hold-down three-electrode electrochemical cell. The sample was placed on the bottom plane of the cell and pressed down with a beaker. The working electrolyte in the tests was 3% NaCl solution. The auxiliary electrode was made of platinum. Contact of the silver chloride reference electrode with the working electrode was carried out using a Luggin capillary. The potential sweep rate was 3 mV/s.

Mass and depth corrosion parameters were determined using polarization diagrams. Values of taffel coefficients of anode (a_a, b_a) and cathode (a_k, b_k) branches of polarization diagram were determined by method of curve approximation. Experiments were performed on an Elins P-30J potentiostat.

3 samples of 09G2S steel were used as the working electrode:

- sample not tested for low-cycle fatigue;
- sample after testing for low-cycle fatigue without destruction (the number of cycles is 6750);
- destroyed sample (the number of cycles before destruction is 9000).

As a result of approximation of polarization diagrams, taffel constants of anode (a_a, b_a) and cathode (a_k, b_k) branches were determined, then corrosion current density (i_k), mass (K_m) and depth (P) corrosion indices were calculated.

3 Results and discussion

The results of the non-low cycle fatigue studies are presented in Table 1. Figures 3 and 4 show polarization patterns at points 7 and 11 as examples.

Table 1. Results of polarization tests on the sample without low cycle fatigue tests.

Point No.	a_a	b_a	$a_к$	$b_к$	$i_к$, A/m^2	k_m, $g/m^2hr.$	$П$, $mm/year$
1	13.1	3.23	-28.25	-29.71	0.0024	0.003	0.0028
2	106.94	97.56	-58.74	-65.96	0.00041	0.0004	0.0005
3	21.13	11.94	-29.04	-33.7	0.0020	0.002	0.0023
4	14.03	6.09	-33.63	-38.61	0.0033	0.003	0.0038
5	10.85	3.56	-29.97	-37.71	0.0015	0.002	0.0017
6	48.39	41.32	-73.87	-81.72	0.0016	0.002	0.0019
7	62.15	57.07	-68.53	-76.98	0.0081	0.008	0.0094
8	50.34	43.78	-62.2	-70.76	0.0014	0.001	0.0016
9	16.67	8.84	-20.5	-27.84	0.0010	0.001	0.0012
10	33.82	21.69	-42.3	-46.72	0.0001	0.0001	0.0001
11	72.72	57.92	-73	-78.1	0.0000043	0.000004	0.000005

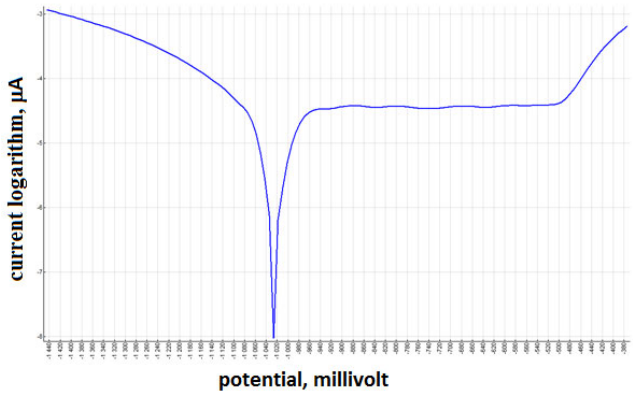

Fig. 3. Polarization diagram of a sample not subjected to low cycle fatigue tests at point 7.

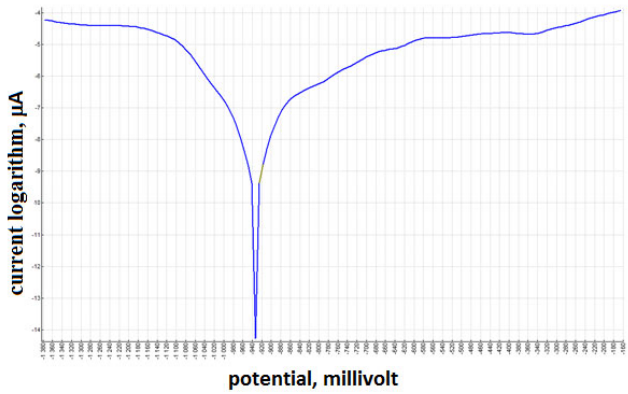

Fig. 4. Polarization diagram of a sample not subjected to low cycle fatigue tests at point 11.

The results of polarization studies on the sample after low cycle fatigue tests with 6750 cycles are presented in Table 2. Figures 5 and 6 show polarization patterns at points 3 and 5 as examples.

Table 2. Results of polarization tests on the sample after low cycle fatigue tests (number of cycles is 6750).

Point No.	a_a	b_a	$a_к$	$b_к$	$i_к$, A/m^2	k_m, $g/m^2hr.$	$П$, $mm/year$
1	54.54	49.88	-68.41	-77.67	0.0078	0.008	0.009
2	11.51	4.21	-38.57	-44.3	0.0045	0.005	0.005
3	34.9	30.42	-32.41	-39.62	0.0498	0.052	0.058
4	76.22	71.25	-91.51	-102	0.0013	0.001	0.001
5	108.13	87.53	-97.11	-99.57	0.0000004	0.0000004	0.0000004
6	38.31	25.62	-27.19	-32.25	0.000232	0.0002	0.0003
7	40.39	32.77	-60.92	-67.13	0.0034	0.004	0.004
8	43.56	27.35	-46.13	-47.77	0.0000288	0.00003	0.00003
9	64.77	60.73	-89.36	-99.93	0.0064	0.007	0.007
10	51.77	43.24	-110.1	-117	0.00038	0.0004	0.0004
11	71.72	66.95	-158.2	-171.3	0.00174	0.002	0.002

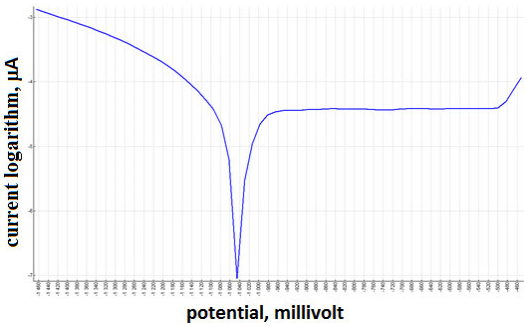

Fig. 5. Polarization diagram of the sample after low cycle fatigue tests with 6750 cycles at point 3.

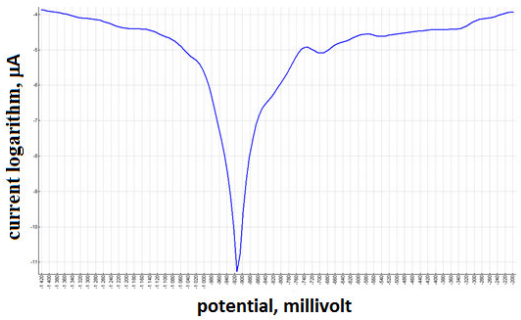

Fig. 6. Polarization diagram of the sample after low cycle fatigue tests with 6750 cycles at point.

It can be seen from the polarization tests that at point 3 the corrosion rate of the steel was an order of magnitude higher than the average values for the length of the sample. This probably indicates a change in the structure of the metal at a given point and the accumulation of damage.

The third sample was tested for low cycle fatigue to failure (number of cycles to failure is 9000). The appearance of the destroyed sample is shown in figure 7. The results of polarization studies on the degraded sample are presented in Table 3. Figures 7 and 8 show polarization patterns at points 6 and 11 as examples.

Fig. 6. Sample after destruction.

Table 3. Results of polarization tests on the destroyed sample.

Point No.	a_a	b_a	$a_к$	$b_к$	$i_к$, A/m^2	k_m, $g/m^2hr.$	$П$, $mm/year$
2	26.53	20.25	-40.24	-47.09	0.012	0.013	0.0142
6	29.5	22.34	-45.47	-52.36	0.0034	0.004	0.0041
11	64.95	52.8	-91.28	-97.45	0.0000085	0.00001	0.00001

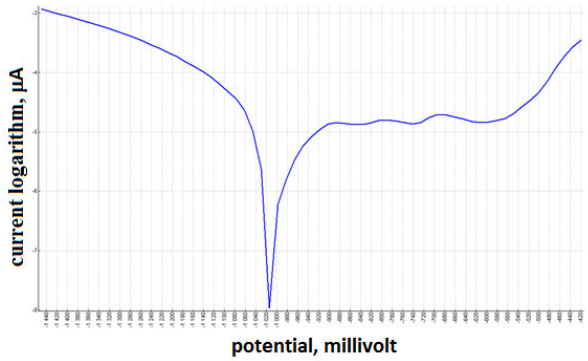

Fig. 7. Polarization diagram of the destroyed sample at point 6.

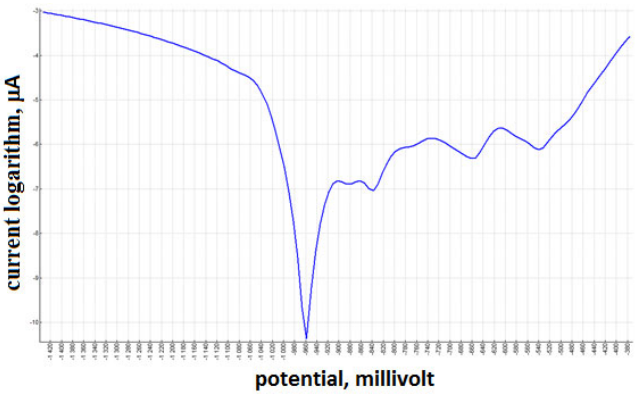

Fig. 8. Polarization diagram of the destroyed sample at point 11.

Analyzing the results obtained for the destroyed sample, it can be seen that at the site of destruction of the sample, the corrosion rate determined by the potentiodynamic method is maximum and an order of magnitude higher than the average values for the length of the sample. This confirms the assumption that it is possible to predict metal destruction sites during cyclic loading using polarization studies.

In order to finally investigate the possibility of applying the above-described technique for predicting metal fracture sites during mechanical loading using polarization studies, it was decided to bring the previously examined sample with the number of cycles 6750 to

fracture. Earlier studies showed that the maximum corrosion rate was recorded at point 3. Therefore, if the destruction of the sample occurs at this point or zones close to it, then the proposed method can be considered quite reliable.

To visualize the destruction zone, the test sample was marked into 11 zones corresponding to polarization studies using a marker. Destruction of the sample occurred when 11,200 loading cycles were reached in the zone adjacent to point 3. The destroyed sample and the destruction zone are shown in Figure 9.

Fig. 9. Destroyed sample and destruction zone.

The obtained result proves the assumption of direct dependence of increased corrosion rate and places of destruction during cyclic loading of metal samples.

4 Conclusion

As a result of the studies, the following conclusions can be drawn:

- it has been experimentally established that in some zones of samples of the metal under study during cyclic loading, the corrosion rate is an order of magnitude higher than the average values, which may indicate the maximum level of accumulated damage. The above relationship can serve as an indicator for identifying possible foci of subsequent destruction;
- it was shown that the destruction of samples during their cyclic loading is observed practically in those zones for which the maximum corrosion rate was recorded during polarization studies.

References

1. A.O. Umeozokwere, I. U. Mbabuike, B.U. Oreko, D.T. Ezemuo, Journal of Scientific and Engineering Research **3(1)**, 34-43 (2016).
2. Y. Luchun, D. Yupeng, L. Zhaoyang, G. Kewei, Science and Technology of Advanced Materials **21(1)**, 359-370 (2020).
3. H. Wang, Ch. Yu, S. Wang, J. Gao, Int. J. Electrochem. Sci. **10,** 1169-1185 (2015).
4. A. Cueli, Y. Adames, O. Latypov, Avances en Ciencias e Ingeniería **11(3)**, 33 (2020).
5. E.V. Khasbutdinova, E.A. Naumkin, A.A. Elizariev, P.A. Kulakov, A.V. Rubtsov, Journal of Physics: Conference Series **1515**, 042056 (2020).
6. V.I. Bolobov, I.V. Zhuikov, G.G. Popov, Oil and gas business **21(4)**, 109-120 (2023).
7. F. Hasan, J. Iqbal, F. Ahmed, Engineering Failure Analysis **14(5),** 801-809 (2007).